THE JOURNAL OF BIOLOGICAL CHEMISTRY VOL. 285, NO. 23, pp. 17693–17700, June 4, 2010

Oral Administration of a GSK3 Inhibitor Increases Brain Insulin-like Growth Factor I Levels*[S]

Received for publication, December 22, 2009, and in revised form, March 22, 2010 Published, JBC Papers in Press, March 29, 2010, DOI 10.1074/jbc.M109.096594

Marta Bolós, Silvia Fernandez, and Ignacio Torres-Aleman[1]

From the Cajal Institute, Consejo Superior de Investigaciones Científicas, and Ciberned, Madrid 28002, Spain

Reduced brain input of serum insulin-like growth factor I (IGF-I), a potent neurotrophic peptide, may be associated with neurodegenerative processes. Thus, analysis of the mechanisms involved in passage of blood-borne IGF-I into the brain may shed light onto pathological mechanisms in neurodegeneration and provide new drug targets. A site of entrance of serum IGF-I into the brain is the choroid plexus. The transport mechanism for IGF-I in this specialized epithelium involves the IGF-I receptor and the membrane multicargo transporter megalin/LRP2. We have now analyzed this process in greater detail and found that the IGF-I receptor interacts with the transmembrane region of megalin, whereas the perimembrane domain of megalin is required for IGF-I internalization. Furthermore, a GSK3 site within the Src homology 3 domain of the C-terminal region of megalin is a key regulator of IGF-I transport. Thus, inhibition of GSK3 markedly increased internalization of IGF-I, whereas mutation of this GSK3 site abrogated this increase. Notably, oral administration of a GSK3 inhibitor to adult wild-type mice or to amyloid precursor protein/presenilin 1 mice modeling Alzheimer amyloidosis significantly increased brain IGF-I content. These results indicate that pharmacological modulation of IGF-I transport by megalin may be used to increase brain availability of serum IGF-I. Interestingly, GSK3 inhibitors such as those under development to treat Alzheimer disease may show therapeutic efficacy in part by increasing brain IGF-I levels, an effect already reported for other neuroprotective compounds.

Although all organs in the body produce insulin-like growth factor I (IGF-I),[2] this abundant circulating growth factor is taken up by target tissues such as muscle and brain (1, 2). The functional significance of this apparently redundant mechanism is not understood. Nevertheless, the neuroactive role of serum IGF-I has been widely documented (3). Probably, its relation to cognition is the most striking aspect (4). Based on these observations, we postulated that brain input of circulating IGF-I may be compromised in different brain diseases (5). This has been recently confirmed by others (6, 7). Thus, enhancing IGF-I input to the brain may be of therapeutic value in different neurodegenerative conditions.

A site of entrance of serum IGF-I into the brain is across the choroid plexus (1, 8). The blood-CSF barrier provided by choroid plexus epithelial cells is functionally similar to the blood-brain barrier formed by brain endothelial cells (9). All transport mechanism at these barriers relay on specific carrier proteins. After IGF-I binds to its membrane receptor, both are internalized through an endocytic pathway involving complex protein-protein interactions (10). In choroid plexus epithelium, where the IGF-I receptor (IGF-IR) is abundantly expressed (11), we previously observed that the IGF-IR interacts with the membrane protein megalin/LRP2 to transport serum IGF-I into the brain. Choroid plexus expression of a megalin small interfering RNA or of a dominant negative IGF-IR resulted in blocked transport of IGF-I into the CSF, indicating that both are needed for this transport (12). Based on these observations, we postulated that regulation of choroid plexus megalin/IGF-IR activity could provide a means to increase the amount of serum IGF-I transferred to the CSF and in this way reach its target areas in the brain (12). However, the mechanisms regulating IGF-I transport through megalin are not known. Although the extracellular N-terminal portion of megalin is involved in binding of multiple ligands (13), the cytoplasmic C terminus probably constitutes an important regulatory site because it is modulated by different intracellular signaling pathways and interacts with many docking proteins (14).

In this regard, a GSK3 site was recently described in the intracellular cytoplasmic tail of megalin (15). This site appears constitutively phosphorylated by GSK3 and regulates the cell membrane location of megalin. Thus, at least in theory, inhibition of GSK3 could modulate the transport activity of megalin by modulating its membrane availability. Because IGF-I inhibits GSK3β through its canonical phosphatidylinositol 3-kinase/protein kinase B signaling pathway, we focused on this kinase as a potential means to modulate the entrance of serum IGF-I into the brain through modulation of choroid plexus megalin. Furthermore, inhibition of GSK3 has turned out to be a promising new strategy in Alzheimer disease therapy as GSK3 is a tau-kinase involved in tauopathy and probably also in amyloid accumulation (16). Because IGF-I is also a potential beneficial factor in Alzheimer disease (17, 18), a combined effect of both GSK inhibition and IGF-I could constitute a new therapy for Alzheimer disease. We now report that inhibition of this GSK3

* This work was supported by Comunidad Autonoma de Madrid (Neurodegs consortium) and Ciberned.

[S] The on-line version of this article (available at http://www.jbc.org) contains supplemental Fig. 1.

[1] To whom correspondence should be addressed: Cajal Institute, Avda. Dr. Arce 37, Madrid 28002, Spain. E-mail: torres@cajal.csic.es.

[2] The abbreviations used are: IGF-I, insulin-like growth factor I; IGF-IR, IGF-I receptor; bIGF-I, biotinylated IGF-I; hIGF-I, human IGF-I; CSF, cerebrospinal fluid; GSK, glycogen synthase kinase; APP, amyloid precursor protein; PS1, presenilin 1; GFP, green fluorescent protein; SH3, Src homology 3; WB, Western blotting; ELISA, enzyme-linked immunosorbent assay; GAPDH, glyceraldehyde-3-phosphate dehydrogenase; MDCK, Marin-Darby canine kidney; HBSS, Hanks' balanced salt solution; qPCR, quantitative PCR.

site in the cytoplasmic domain of megalin markedly increases brain IGF-I levels.

EXPERIMENTAL PROCEDURES

Animals and Reagents—Postnatal day 7 Wistar rats, wild-type C57BL/J6 (2–3 months old; Harlan, Barcelona, Spain) and APP/PS1 (2–3 months old, C57BL/J6 background) male mice (a gift from Dr. P. Mouton, National Institutes of Health) were used. At this age, APP/PS1 mutants initiate amyloid plaque deposition in the brain (data not shown). Animals were kept under light/dark conditions following European Union guidelines (directive 86/609/EEC) and handled according to institutionally approved procedures. Water and food were provided *ad libitum*. All efforts were made to minimize suffering and the number of animals. Antibodies against the IGF-IR and megalin were from Santa Cruz Biotechnology (Santa Cruz, CA). Anti-Ser(P)^{9} GSK3β was from Cell Signaling. Anti-Tyr(P)^{279}/Tyr(P)^{216}GSK3 were from Millipore. Anti-GSK3β was from BD Transduction Laboratories. Anti-digoxigenin from was Roche Applied Science. Anti-green fluorescence protein (GFP) was from Invitrogen, and anti-β-actin was from Sigma. A streptavidin-biotin horseradish peroxidase complex was from Amersham Biosciences. Biotin-IGF-I was from IBT. The GSK3 inhibitor NP12 was a gift from Noscira (Spain). The GSK3 inhibitor 1 was from Calbiochem. Bovine serum albumin (Sigma) was labeled with digoxigenin-3-*O*-methylcarbonyl-ϵ-aminocaproic acid-*N*-hydroxysuccinimide ester following the manufacturer's instructions (Roche Applied Science). A fluorescent membrane marker FM-4-64 X (Molecular Probes) was used in confocal analysis.

Plasmids—A cDNA coding for the two perimembrane extracellular cysteine-rich domains, the transmembrane part, and the entire cytoplasmic region of the megalin gene (herein called mini-megalin; a gift from L. Larsson, Sweden) was cloned in a pEGFP-N1 vector using EcoRI/KpnI restriction sites. Primers used were 5′-AGA CCC AAG CTT GGA ATT CCC ACC-3′ and 3′-CTT CTG AGA CTC CAT GGC TTA AGA-5′ (mini-megalin–GFP). Using mini-megalin–GFP as a template, C-terminal mutants of megalin were constructed with progressive truncations. The 5′–3′ primer of mini-megalin–GFP was the same for all mutants, whereas the 3′–5′primer, including the KpnI restriction site, differed. In a first mutant, the last three residues corresponding to a PDZ binding domain were deleted (ΔPDZ); the primer used was 3′-GAA CAA TTT CTC CAT GGA CTT CAT-5′. In the next, an Src homology 3 site was eliminated (ΔSH3 PDZ) using the primer 3′-TTC CTT TCA CAC CAT GGC TGT GGT-5′. A third C-terminal mutant (ΔNPXY SH3 PDZ) using the primer 3′-TTC GTC GGG TAC CAT GGA CTT TTG-5′ was generated in which an NPXY site was deleted. An N-terminal mutant (ΔExtracellular) lacking 80 residues of N-terminal mini-megalin was constructed using the primers 5′-GCG TTT TCA AAA GGA TCC TCT CCA-3′ and 3′-CTT CTG AGA CTC CAT GGC TTA AGA-5′.

Immunoassays—For Western blotting (WB), cultured cells were washed once with ice-cold phosphate-buffered saline and lysed in PIK buffer (150 mM NaCl, 20 Mm Tris-HCl, pH 7.4, 1% Nonidet P-40, 1 μg/ml aprotinin, 1 μg/ml leupeptin, and 1 mg/ml phenylmethylsulfonyl fluoride). For cell fractionation cells were lysed with $NaHCO_3$ 5 mM, 1 μg/ml aprotinin, 1 μg/ml leupeptin, and 100 μM phenylmethylsulfonyl fluoride. The cell lysate was cleared by centrifugation at 1000 × *g* for 10 min, and membranes were obtained by centrifugation of the supernatant for 1 h at 100,000 × *g*. After running the samples in acrylamide gels, proteins were transferred (Inmobilon; Bio-Rad) and membranes incubated with either streptavidin-biotinylated horseradish peroxidase for 3 h in experiments with biotinylated IGF-I or overnight with the corresponding primary antibodies (1:1000) at 4 °C. Thereafter, membranes were washed and incubated with secondary antibodies (1:10,000) for 1 h. Membranes were then washed three times with Tween-TBS/10 min and developed with ECL (Amersham Biosciences). To normalize for protein load, membranes were reblotted (Re-Blot; Chemicon) and incubated with either anti-β-actin for cell lysates or anti-IGF-IR for cell membrane fractions. When needed, levels of the protein under study were expressed relative to protein load in each lane as determined by β-actin content. Different exposures of each blot were collected to ensure linearity and to match control levels for quantification. Densitometric analysis was performed using Quantity One software (Bio-Rad). A representative blot is shown from a total of at least three independent experiments. For immunoprecipitation, cells were lysed with PIK buffer and centrifuged at 22,000 × *g* for 20 min. Supernatants were incubated with primary antibody overnight. Protein A-agarose (Invitrogen) was added to the antigen-antibody mixture and incubated with gentle agitation overnight. The immunoprecipitate was washed three times with the same lysis buffer, resuspended in 2.5× SDS loading buffer, electrophoresed, transferred to the nitrocellulose membrane, and analyzed by WB.

IGF-I ELISA—Human and murine IGF-I assays were performed as described (4). In the latter case, 96-well plates (Costar) were coated with monoclonal anti-mouse IGF-I antibody (mAb 791, 100 μl/well; R&D Systems, Minneapolis, MN) overnight at 4 °C. Between each step, the plates were washed three times with 200 μl of wash solution (0.05% Tween 20 in phosphate-buffered saline, pH 7.4). Thereafter, 300 μl of blocking solution (phosphate-buffered saline, pH 7.4 + 5% Tween + 5% sucrose + 0.05% azide) was added to each well for 1–2 h at room temperature. Afterward, 100 μl of sample or standard curve was added and incubated overnight at 4 °C. After washing, 100 μl of biotinylated anti-mouse IGF-I antibody was added (BAF-791; R&D Systems). Finally, after incubating with 100 μl of streptavidin-horseradish peroxidase (Amersham) for 2 h at room temperature with constant shaking, 200 μl of OPD (Sigma) was added and incubated for 20–30 min at room temperature. Absorbance at 450 nm was measured in an ELISA plate reader. Using this assay, we did not detect human IGF-I (4). Human IGF-I (hIGF-I) was measured with a commercial ELISA for hIGF-I (DSL) following the manufacturer's instructions (sensitivity of 13 ng/ml). In this assay, control wild-type mice receiving the vehicle had undetectable serum levels of hIGF-I (4).

Quantitative PCR (qPCR)—RNA from cortex and liver was extracted using the RNAspin mini kit (GE Healthcare). The DNA of the samples was obtained from 1 μg of RNA with a high capacity cDNA reverse transcription kit (Applied Biosystems) using the PCR program recommended by the manufacturer.

IGF-I and GAPDH primers used were from Applied Biosystems. All samples were diluted 1:2 and run in triplicate. Standard curves for IGF-I and GAPDH with concentrations 1, 0.5, 0.25, and 0.125 μg were used to quantify IGF-I mRNA. GAPDH was used as an internal control. Universal Taqman master mix from Applied Biosystems was used. Results were analyzed with the 7000 system SDS software (Applied Biosystems).

Cell Cultures and Transfections—Madin-Darby canine kidney (MDCK) cells, an epithelioma that maintains the main functional characteristic of a sealed epithelium similar to the choroid plexus (including high electrical resistance when forming a sealed monolayer), were used for molecular analyses because they are easier to manipulate and express low megalin levels. MDCK cells were plated in 12-well plates (40,000 cell/well) in Dulbecco's modified Eagle's medium (Invitrogen)/F-12 supplemented with 5% fetal bovine serum and kept at 37 °C with 5% CO_2. Cells were transfected 24 h later. The ratio of DNA to transfection reagent (LT-1; Mirus, Bionova, Spain) was 1 μg:3 μl. After 24 h, the percentage of cells transfected was 85–95%, as assessed with a GFP vector. In the day of the experiment, medium was replaced with fresh Dulbecco's modified Eagle's medium/F-12 without serum. Two h later, cells were treated with NP12 (100 μM), biotin-IGF-I (IBT), digoxigenin-albumin (1 μg/ml) for 1 h, 20 min, or 3 h, respectively. Cells were then lysed. In experiments to visualize the mutants within the cells, coverslips were stained with the membrane marker FM 4-64X (5 μg/ml; Molecular Probes) in ice-cold HBSS for 1 min. The stain was fixed with ice-cold 4% paraformaldehyde in HBSS, placed on ice 10 min. Coverslips were rinsed three times with HBSS and mounted in HBSS, sealed, and visualized with confocal microscopy (Leica, Germany).

Choroid plexus cells were cultured as described (12). Briefly, choroid plexus was dissected, digested with DNase and protease (both from Sigma), and filtered. Cells were plated at 150,000 cells/well in laminin- (10 μg/ml; Sigma) coated 12-well plates and grown to confluence for about 7 days. A double-chamber system mimicking the blood-CSF interface was used in transcytosis experiments, as described (17). Cells were plated in 0.4-μm well inserts (Millipore) coated with laminin (10 μg/ml) at 80,000 cells/insert. To determine that the monolayer of choroid plexus epithelial cells formed a barrier, electrical resistance was measured with a voltmeter (Millicell-Electrical Resistance System, Millipore). When resistance reached a value of ~96 ohms × cm, we considered the monolayer sealed. Under these conditions, no leakage of inulin, a marker of intercellular passage, was seen (17). On the day of the experiment, fresh medium without serum was added, and 4 h later either 1 μg/ml digoxigenin-albumin or 1 μg/ml biotinylated IGF-I added to the lower chamber ("blood side"). The medium was collected 24 h later.

In Vivo Experiments—Adult male wild-type (C57BL/J6) and APP/PS1 mice were orally administered NP12 (200 mg/kg) for 5 days using a gastric cannula. 0.5 h after the last dose, mice were killed by CO_2 suffocation. Serum and CSF were collected (from cisterna magna) and perfused with saline through a cardiac cannula, and the choroid plexus, cortex, and liver were dissected. A minimum of 6 animals/group was used (see legends for further details). In another series of experiments, wild-type mice received one dose of NP12 (orally administered as above) or the vehicle, and 1–2 h later animals were intraperitoneally injected with recombinant hIGF-I (1 μg/g dissolved in saline). Two h later, the CSF was collected through the cisterna magna (~10 μl) as described (12), extracted in Sep-Pak cartridges to eliminate protein interferences, lyophilized, and assayed by human ELISA after reconstitution in 55 μl of phosphate saline.

Statistics—Data are expressed as means ± S.D. Differences between groups were analyzed by one-way analysis of variance. Post hoc comparisons between two groups were done with Student's *t* test. A $p < 0.05$ was considered significant.

RESULTS

Role for the Cytoplasmic Tail of Megalin in IGF-I Internalization—We mutated the perimembrane region and cytoplasmic tail of megalin to analyze their role in IGF-I internalization. A construct comprising the full C-terminal intracellular region of megalin, the perimembrane domain, and two of the extracellular ligand-binding moieties was used (19). This "mini-megalin" construct retained the ability to co-immunoprecipitate with the IGF-IR in MDCK cells (Fig. 1*A*) similarly to native megalin from choroid plexus (Fig. 1*B*). Different mini-megalin truncations comprising the C-terminal region and the extracellular perimembrane region (supplemental Fig. 1*A*) co-immunoprecipitated with IGF-IR (Fig. 1*A*). These mutants were present in the membrane, as determined by their co-localization with a membrane-specific dye in confocal microscopy (Fig. 1*C*) and by WB of the membrane fraction (Fig. 1*D*, *right blots*).

Mini-megalin also mimicked native megalin in enhancing IGF-I internalization. Expression of mini-megalin increased IGF-I internalization in MDCK cells over that seen in GFP-transfected cells ($p < 0.05$; Fig. 1*D*). Mini-megalin mutants lacking up to the SH3 region of the C terminus were able to internalize IGF-I. However, a mutant lacking the outer perimembrane region and another one lacking most of the C terminus did not internalize IGF-I (Fig. 1*D*, *left blots*). Lack of internalization of IGF-I was not due to defective insertion in the cell surface because WB of the GFP-tagged mutants showed their presence in the membrane fraction (Fig. 1*D*, *right blots*). This confirmed the co-localization seen with a membrane marker through confocal microscopy (Fig. 1*C*). Collectively, these data indicate that the C-tail portion of megalin participates in internalization of IGF-I, whereas it is not essential to interact with the IGF-IR.

GSK3 Site in the Cytoplasmic Tail of Megalin Modulates IGF-I Transport—Inhibition of GSK3 increases the levels of megalin in the cell surface by dephosphorylation of a GSK site in the C terminus of megalin (15). Hence, we determined whether IGF-I internalization would be affected. We tested several commercially available GSK3 inhibitors and found that NP12, a novel inhibitor currently in clinical testing for Alzheimer disease (21), was the most potent. This compound markedly stimulated internalization of IGF-I by MDCK cells transfected with mini-megalin and at the same time increased the amount of megalin present in the cell surface (Fig. 2*A*). Other GSK inhibitors were less potent (Fig. 2*A* and data not shown).

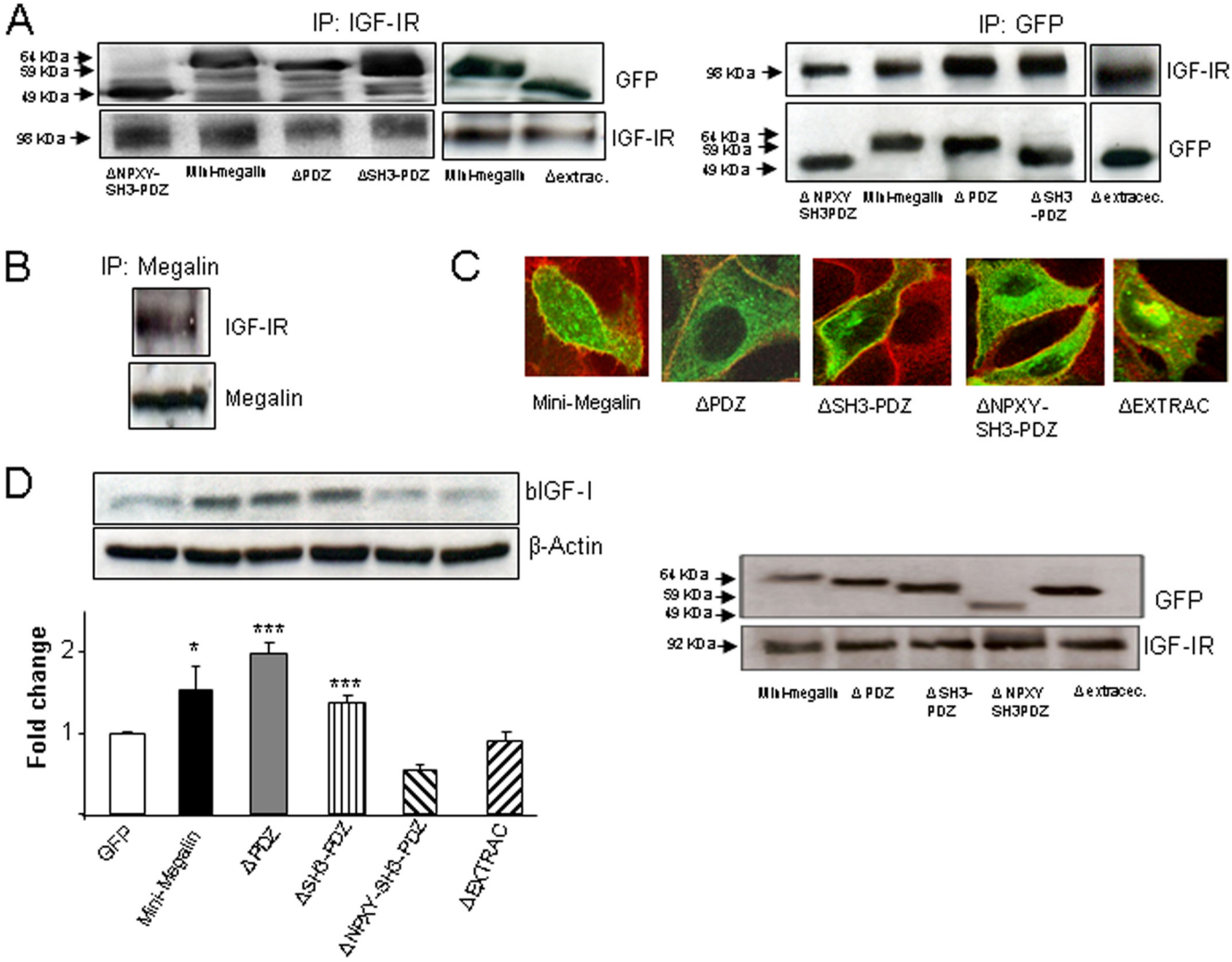

FIGURE 1. **Different regions of megalin are differentially involved in IGF-I transport.** *A*, C terminus and extracellular perimembrane regions of megalin are not involved in the interaction with IGF-IR. Megalin mutants with progressive truncations of the C-terminal domain or the extracellular region closer to the membrane and tagged with GFP interacted with IGF-IR. MDCK cells were transfected with different megalin mutants (for details, see supplemental Fig. 1) and immunoprecipitated (*IP*) with either anti-IGF-I (*left blots*) or anti-GFP antibodies (*right blots*). WB of GFP (*left*) or IGF-IR (*right*) indicated that both proteins co-immunoprecipitate. Membranes were reblotted with anti-IGF-IR or anti-GFP as a control. Representatives blots are shown ($n = 3$). *B*, native megalin in choroid plexus co-immunoprecipitates with IGF-IR. Choroid plexus extracts were immunoprecipitated with anti-megalin antibody and revealed with anti-IGF-IR by WB ($n = 3$). *C*, megalin mutants lacking the C-terminal or the extracellular perimembrane region localize to the cell membrane. MDCK cells were transfected, and the presence of the mutants in the membrane was analyzed by co-localization with the fluorescent membrane dye FM 4-64X. Co-localization is noted as a *yellowish* signal. *D*, perimembrane region of megalin is required for IGF-I internalization. Although mini-megalin and mutants lacking either the PDZ or the PDZ+SH3 domain efficiently internalized bIGF-I, mutants lacking either the intracellular (Δ*NPXY/SH3/PDZ*) or the extracellular perimembrane regions (Δ*Extracellular*) did not show activity (*left blot*). All GFP-tagged mutants were present in the cell surface, as determined by WB of membrane fraction extracts. WB of IGF-IR was performed as a control of the membrane fraction (*right blots*). Representative blots and quantitation histograms are shown ($n = 3–6$; *, $p < 0.05$; ***, $p < 0.001$ *versus* GFP-transfected MDCK cells). *Error bars*, S.E.

Either point mutation of the GSK3 site (ΔGSK3/SH3 mutant) or truncation of the entire region containing this site (ΔSH3/PDZ) in the C terminus of mini-megalin fully abrogated the effect of NP12 (Fig. 2*B*). This confirms the involvement of this site in modulating IGF-I transport. Similar effects were seen when using primary choroid plexus cells in double-chamber cultures mimicking the *in vivo* blood-to-brain transport process (18). Transcytosis of IGF-I across the epithelial monolayer was markedly enhanced after treatment with NP12. Transport of biotinylated IGF-I (bIGF-I) placed in the lower chamber (corresponding to the blood side in the *in vitro* system) to the upper chamber (corresponding to the CSF side) was markedly increased by NP12 ($p < 0.01$ *versus* control; Fig. 2*C*). Because megalin transports many other blood proteins across the choroid plexus, we tested whether NP12 affected transcytosis activity of megalin in general using albumin as an alternative cargo (22). As seen in Fig. 2*D*, no effect of NP12 was observed in transcytosis of digoxigenin-labeled albumin in the double-chamber system. As already described (17), using the same experimental setting IGF-I increased transcytosis of albumin. This confirms that NP12 was inactive as the *in vitro* system allows transcytosis of albumin when receiving an appropriate stimulus (*i.e.* IGF-I).

Inhibition of GSK3 Increases Brain IGF-I Levels—To determine the *in vivo* significance of these observations, we treated adult C57BL/J6 male mice during 5 days with NP12 (200

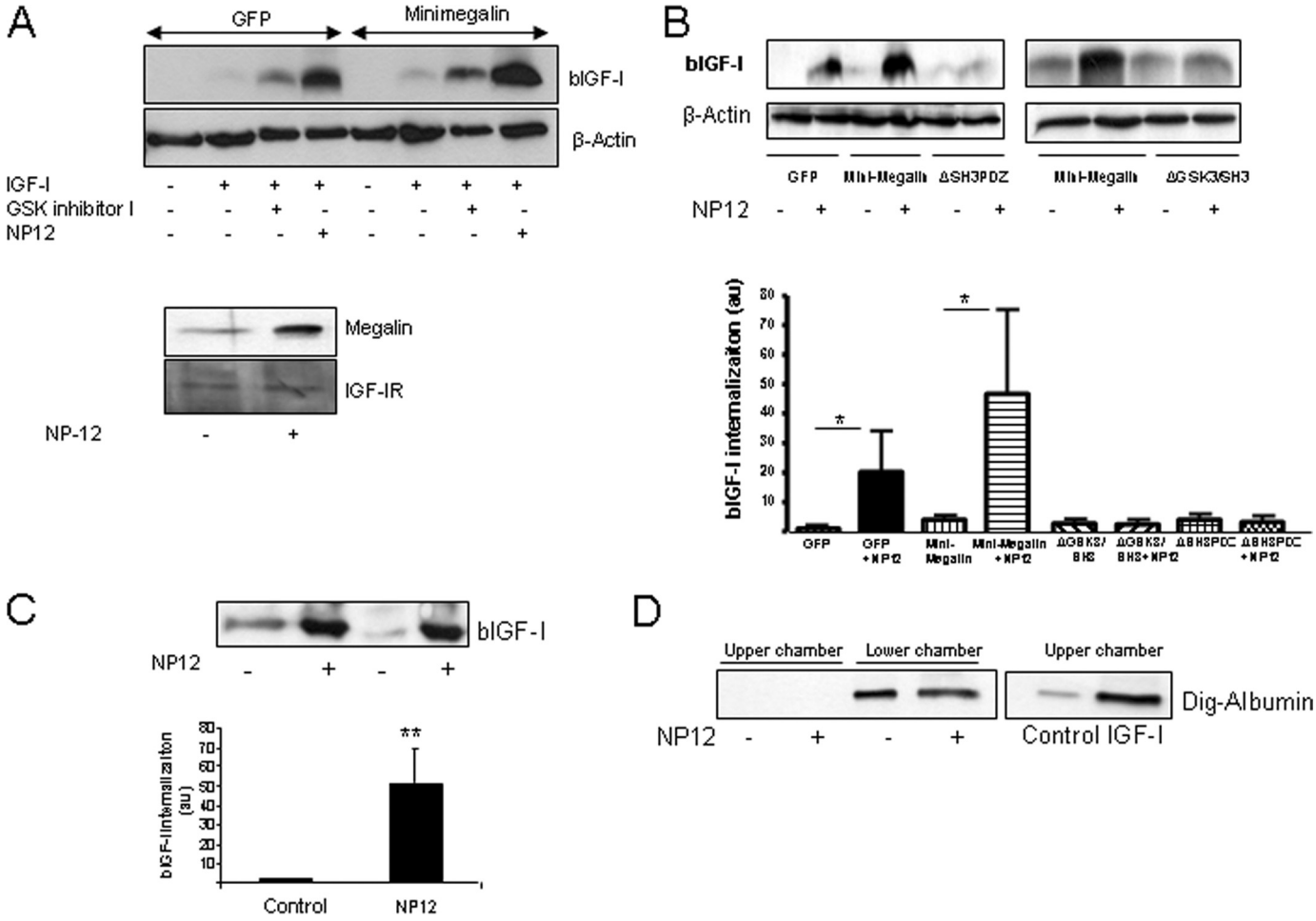

FIGURE 2. **Inhibition of GSK increases transport of IGF-I.** *A*, MDCK cells transfected with either GFP or mini-megalin and exposed to a GSK inhibitor (200 μM, GSK inhibitor I; Calbiochem) or NP12 (100 μM; Noscira) showed increased internalization of bIGF-I. A representative blot is shown. Membranes were reblotted with anti-β-actin antibody as a loading control ($n = 4$). *Lower blots*, note the increased presence of megalin, but not IGF-IR in the surface of the cell (membrane fraction) after treatment with NP12. *B*, inhibition of GSK3 involves the GSK3 site located at the SH3 region of the C terminus of megalin. Mini-megalin mutants lacking either the entire SH3 region (*SH3*) or just the GSK3 site (*GSK3*) did not show increased bIGF-I in response to GSK3 inhibition with NP12. Representative blots and quantitation histograms are shown ($n = 6$; *, $p < 0.05$ *versus* respective controls). *C*, transcytosis of IGF-I across the choroid plexus monolayer is markedly increased by NP12. Significantly greater amounts of bIGF-I were detected in the CSF side (upper chamber) of the double-chamber system (for details, see "Experimental Procedures"). Representative blots of upper-chamber supernatants and quantitation histograms are shown ($n = 5$; **, $p < 0.01$). *D*, transcytosis of digoxigenin-labeled albumin (*Dig-albumin*) is not affected by NP12. No digoxigenin-labeled albumin was detected in the upper chamber, whereas it was readily detected in the lower chamber. IGF-I did modulate transcytosis of albumin, as already published (12). *Error bars*, S.E.

mg/kg/day, orally) or the vehicle and determined brain levels of IGF-I. As shown in Fig. 3*A*, treatment with NP12 significantly increased brain IGF-I levels ($p < 0.05$). At the same time, serum IGF-I levels were modestly, but significantly reduced (Fig. 3*B*). IGF-I levels in the CSF were not significantly modified (Fig. 3*C*). Levels of IGF-I mRNA in the liver of treated animals remained unaltered, as determined by qPCR (Fig. 3*D*). Notably, brain IGF-I mRNA was reduced (Fig. 3*E*). In NP12-treated animals, GSK3 activity measured by relative levels of Tyr(P) GSK3 (active) and Ser(P) GSK3 (inactive) *versus* total GSK levels in choroid plexus showed a significant ~50% reduction (Fig. 3*F*), whereas brain GSK3 activity was unaffected by treatment (data not shown). Confirming this, treatment with NP12 decreased choroid plexus levels of Ser(P) megalin, indicating that NP12 inhibits GSK3 phosphorylation of megalin (Fig. 3*G*). No effects of treatment were observed on choroid plexus levels of megalin mRNA or in the levels of brain IGF-I receptors as determined by qPCR and WB, respectively (supplemental Fig. 1, *B* and *C*).

Next, we determined whether in APP/PS1 mice, a transgenic model mimicking amyloidosis and cognitive deterioration in Alzheimer disease (23), treatment with NP12 elicited a similar effect as GSK3 inhibitors are currently on clinical trials for Alzheimer disease (21). Although NP12 similarly increased brain IGF-I levels in APP/PS1 mice (Fig. 4*A*), no changes in serum IGF-I levels were found (Fig. 4*B*). In contrast, CSF levels of IGF-I were markedly increased by the drug ($p < 0.05$; Fig. 4*C*). In APP/PS1 mice, the levels of IGF-I mRNA in liver (Fig. 4*D*) and brain (Fig. 4*E*) remained unchanged after NP12 treatment. As seen in wild-type mice, no changes in megalin mRNA of brain IGF-IR levels were found after treatment (supplemental Fig. 1, *D* and *E*).

Although in control mice IGF-I levels in the CSF were not altered by NP12 (Fig. 3*C*), in APP/PS1 mice NP12 increased

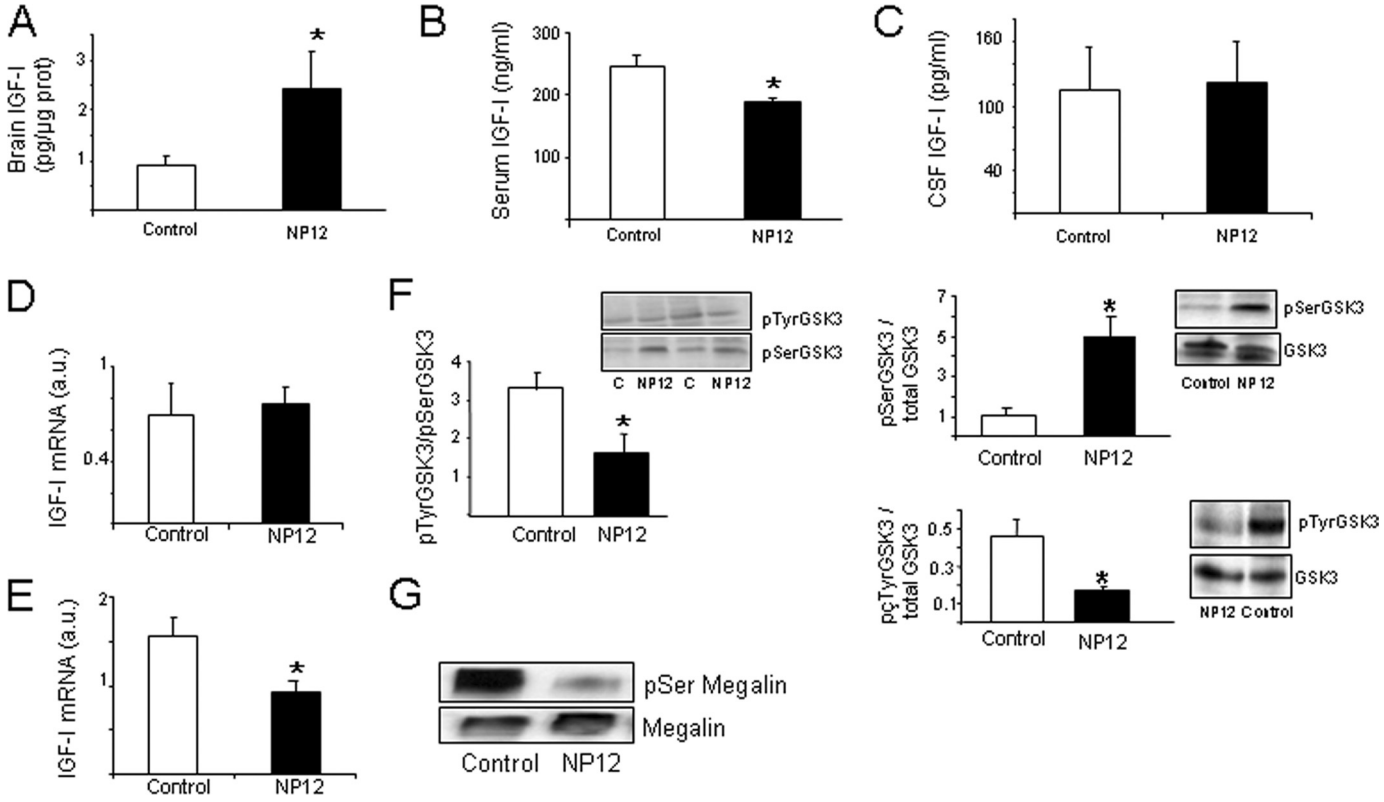

FIGURE 3. ***In vivo* inhibition of GSK3 results in increased brain IGF-I levels.** *A*, levels of IGF-I in brain of mice treated with NP12 for 5 days were significantly increased compared with vehicle-treated animals ($n = 13–15$; *, $p < 0.05$). *B*, after treatment with NP12 serum, IGF-I levels were modestly but significantly decreased ($n = 11$; *, $p < 0.05$). *C*, levels of IGF-I in CSF remained unaffected by NP12 treatment ($n = 9–10$). *D* and *E*, levels of IGF-I mRNA determined by qPCR in liver (*D*) or brain (*E*) were either unchanged or decreased, respectively ($n = 5$; *, $p < 0.05$). *F*, oral administration of NP12 to adult mice resulted in inhibition of GSK3 activity in choroid plexus as determined by analyzing the levels of inactive (*pSerGSK3*) and active (*pTyrGSK3*) kinase in choroid plexus *versus* total GSK levels. The Tyr(P)/Ser(P) as well as the Ser(P)/total and Tyr(P)/total ratios are shown ($n = 6$; *, $p < 0.05$. *C*, control). *G*, levels of Ser(P) megalin in choroid plexus were decreased in mice treated with NP12. Choroid plexus was immunoprecipitated with anti-megalin and blotted with an anti-Ser(P) antibody. Total megalin was also determined. Representative blot is shown (NP12, $n = 9$; control, $n = 5$). *Error bars*, S.E.

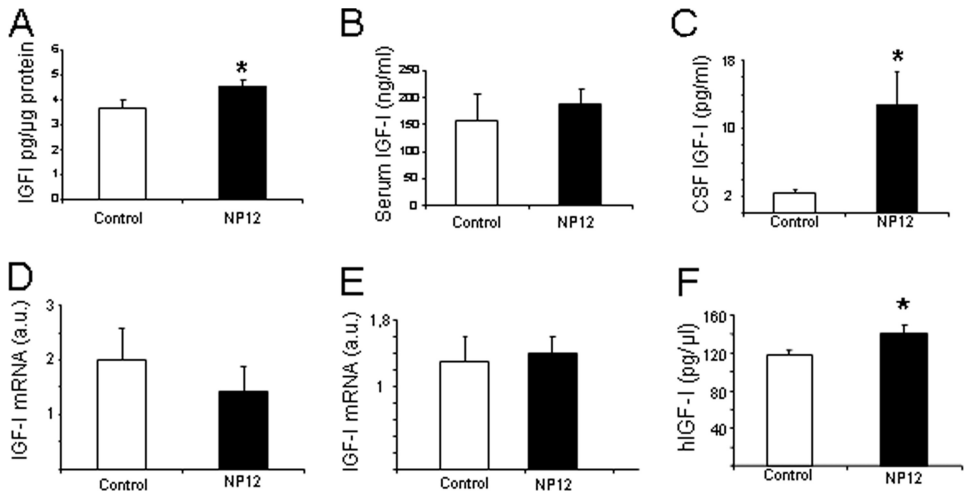

FIGURE 4. **Modulation of IGF-I after inhibition of GSK3 in APP/PS1 mice.** *A*, brain IGF-I levels in APP/PS1 mice treated with NP12 were significantly increased compared with vehicle-treated animals (*, $p < 0.05$). *B*, serum IGF-I in APP/PS1 mice was not changed after NP12. *C*, levels of IGF-I in CSF were greatly increased by NP12 treatment (*, $p < 0.05$). Levels of IGF-I mRNA determined by qPCR in liver (*D*) or brain (*E*) were unchanged ($n = 5–7$ in all experiments). *F*, NP12 ($n = 9$) significantly increases CSF levels of subcutaneously administered hIGF-I (1 μg/g) in wild-type mice compared with vehicle-treated mice ($n = 5$); *, $p < 0.05$. *Error bars*, S.E.

them, suggesting that the drug is facilitating serum-to-CSF traffic of IGF-I. Thus, we performed an additional experiment in wild-type mice to explore this possibility further. We administered hIGF-I to NP12-treated wild-type mice and determined its CSF levels 1–2 h later using an hIGF-I-specific ELISA (4). We observed a small but significant increase in CSF hIGF-I after NP12 (Fig. 4*F*).

DISCUSSION

The present results indicate that megalin/LRP2 may be a suitable target to modulate transport of serum IGF-I into the brain for therapeutic purposes. We found that the perimembrane region of megalin is involved in internalization of IGF-I; deletion of either the extra- or intracellular perimembrane moieties abolished it. In addition, a GSK3 site located in the intracellular C-terminal region modulates transport of IGF-I in a tonic fashion as its inhibition led to increased transcytosis of IGF-I. Hence, systemic inhibition of GSK3 may constitute a feasible way to increase brain IGF-I levels. Intriguingly, increased brain IGF-I has already been seen with other neu-

roprotective compounds such as glatiramer acetate and donepezil (24, 25).

As several GSK3 inhibitors are in the pipeline for clinical use in Alzheimer disease (26), it is possible that their effectiveness relies not only on their ability to diminish tauopathy through GSK3 inhibition, but also to increase brain availability of IGF-I. Indeed, in APP/PS1 mice the drug similarly elicited an increase in brain IGF-I. This growth factor is a potent neuroprotective agent of known efficacy in mouse models of Alzheimer disease (17, 18). Notably, decreased GSK3 activity in brain was observed after IGF-I treatment in mice (17). Therefore, systemic administration of GSK inhibitors will impinge on megalin at the blood-brain barrier and initiate a virtuous cycle whereby increased brain IGF-I will contribute to the therapeutic efficacy of GSK3 inhibition.

These results suggest that the choroid plexus is an important site of entrance of serum IGF-I because megalin is more abundant in this structure than in brain vessels (27). Nevertheless, we cannot rule out the possibility that serum IGF-I enters into the brain also through brain vessels not only through megalin/LRP2 but also through its close relative LRP1 that is abundantly expressed in brain endothelium and interacts with the IGF-IR.[3] At any rate, both APP/PS1 and wild-type mice treated with NP12 showed increased levels of IGF-I in the CSF. However, in the case of wild-type animals, we detected increased blood-to-CSF traffic only after administration of exogenous hIGF-I. Probably this reflects that the changes in endogenous CSF IGF-I levels after NP12 are taking place at a slow pace. But this speculation requires further work.

Megalin is a multicargo transmembrane protein with a large extracellular domain containing multiple binding sites for its numerous ligands and a comparatively shorter intracellular C terminus (28). Megalin is expressed in various cell types and has been shown to interact with a wide diversity of proteins and molecules. We previously reported that the IGF-I receptor in choroid plexus interacts with megalin to transport IGF-I (12). Although upon binding to its receptor, IGF-I is internalized by target cells (10), the interaction of the IGF-I receptor with megalin is probably essential for IGF-I transcytosis across polarized cells such as choroid plexus epithelia. When the intra- and extracellular areas surrounding the transmembrane region of megalin are deleted, co-immunoprecipitation with the IGF-IR is still observed, indicating that this transmembrane region is the only essential moiety. It is not possible to gather a more direct proof of the relevance of the transmembrane region of megalin as its elimination will impede sorting of megalin to the membrane.

However, interaction of megalin with IGF-IR is not sufficient to promote IGF-I internalization. When the perimembrane regions of megalin are removed, IGF-I internalization is abrogated, whereas co-immunoprecipitation with the IGF-IR remains intact. Because IGF-I inhibits GSK3 on target cells, these observations suggest that IGF-I is initially internalized through its receptor and subsequently transported across the polarized cell via interaction of the receptor with megalin through a process involving inhibition of the constitutive phosphorylation of megalin by GSK3. In agreement with this possibility is that inhibition of GSK by NP12 did not increase transcytosis of albumin, another of the many ligands of megalin. Collectively, these findings indicate that a constitutive interaction between the IGF-IR and megalin allows transcytosis of IGF-I through a process that recruits the perimembrane moieties and is modulated by the GSK site at the SH3 cytoplasmic region (supplemental Fig. 1*F*). Therefore, IGF-I may be able to regulate its own transfer across the choroid plexus.

In wild-type mice, administration of NP12 increased brain levels of IGF-I in parallel with decreased brain IGF-I mRNA content. In agreement with this, we recently observed that increased brain IGF-I levels after exercise paralleled decreased brain IGF-I mRNA content.[4] Thus, local synthesis of IGF-I in the brain may be modulated by serum IGF-I input to the brain. Further, as serum IGF-I is elevated in mutant mice lacking IGF-IR in brain (29), and conversely, serum IGF-I is decreased after NP12, brain IGF-I levels may be the result of a balance between local synthesis and serum IGF-I input. In turn, serum IGF-I levels appear to be affected by the amount of serum IGF-I input to the brain. Collectively, this further suggests that the brain is an important target of circulating IGF-I. As renal epithelium also expresses high levels of megalin (13), we cannot rule out that decreased serum levels of IGF-I after NP12 treatment are due not only to increased brain entrance but also to increased renal clearance. This requires further analysis.

As in wild-type mice, NP12 increased brain IGF-I in APP/PS1 transgenic mice, although the increase was smaller. In addition, in mutant mice serum IGF-I and brain IGF-I mRNA remained unchanged whereas CSF IGF-I levels were markedly increased. These different responses to the drug between wild-type and APP/PS1 mice are intriguing. A possible explanation is that there are large differences in basal IGF-I levels between both types of mice. Differences in IGF-I levels in serum, brain, and CSF have been already reported both in Alzheimer disease patients and in mouse models (6, 20, 30–34). For instance, as basal CSF IGF-I levels in APP/PS1 mice are very low, the stimulatory actions of NP12 may be readily seen whereas in normal mice increases in CSF may be smaller and probably more transient and therefore more difficult to detect (see above). Although differences in IGF-I levels between wild-type and Alzheimer disease mice probably reflect the involvement of this growth factor in the disease (17), its analysis is beyond the scope of the present work. At any rate, brain IGF-I levels are increased by NP12 in both types of animals. This supports the possibility that part of the beneficial effects of this drug relies on increased availability of IGF-I in the brain.

In summary, the present results further indicate that choroid plexus megalin is an important mediator of serum IGF-I entrance into the brain and may constitute a feasible therapeutic target. Although modulation of GSK3-dependent phosphorylation of megalin did not affect transport of albumin, other megalin ligands may be affected. As several of the ligands of megalin are carriers of β amyloid, increased brain content of

[3] S. Duflot and I. Torres-Aleman, unpublished observations.

[4] M. Llorens, I. Torres-Aleman, and J. L. Trejo, unpublished observations.

these ligands may contribute to increase β amyloid clearance. This remains to be analyzed.

Acknowledgments—We thank I. Alvarez, L. Guinea, and M. Oliva for skillful technical assistance; Dr. Marzolo (Pontifica Universidad Catolica de Chile) for valuable comments on the manuscript and the megalin GSK mutant; Dr. Larsson (University of Uppsala) for the mini-megalin cDNA; and Noscira (Spain) for the GSK3 antagonist NP12.

REFERENCES

1. Carro, E., Nuñez, A., Busiguina, S., and Torres-Aleman, I. (2000) *J. Neurosci.* **20,** 2926–2933
2. Eliakim, A., Moromisato, M., Moromisato, D., Brasel, J. A., Roberts, C., Jr., and Cooper, D. M. (1997) *Am. J. Physiol. Regul. Integr. Comp. Physiol.* **273,** R1557–R1561
3. Carro, E., and Torres-Aleman, I. (2006) *Keio J. Med.* **55,** 59–63
4. Trejo, J. L., Piriz, J., Llorens-Martin, M. V., Fernandez, A. M., Bolós, M., LeRoith, D., Nuñez, A., and Torres-Aleman, I. (2007) *Mol. Psychiatry* **12,** 1118–1128
5. Davila, D., Piriz, J., Trejo, J. L., Nunez, A., and Torres-Aleman, I. (2007) *Front. Biosci.* **12,** 3194–3202
6. Moloney, A. M., Griffin, R. J., Timmons, S., O'Connor, R., Ravid, R., and O'Neill, C. (2010) *Neurobiol. Aging* **31,** 224–243
7. Sharma, S., Prasanthi, R. P. J., Schommer, E., Feist, G., and Ghribi, O. (2008) *Neurobiol. Dis.* **32,** 426–432
8. Armstrong, C. S., Wuarin, L., and Ishii, D. N. (2000) *J. Neurosci. Res.* **59,** 649–660
9. Chodobski, A., and Szmydynger-Chodobska, J. (2001) *Microsc. Res. Tech.* **52,** 65–82
10. Geary, E. S., Rosenfeld, R. G., and Hoffman, A. R. (1989) *Horm. Metab. Res.* **21,** 1–3
11. Davidson, D. A., Bohannon, N. J., Corp, E. S., Lattemann, D. P., Woods, S. C., Porte, D., Jr., Dorsa, D. M., and Baskin, D. G. (1990) *J. Histochem. Cytochem.* **38,** 1289–1294
12. Carro, E., Spuch, C., Trejo, J. L., Antequera, D., and Torres-Aleman, I. (2005) *J. Neurosci.* **25,** 10884–10893
13. Barth, J. L., and Argraves, W. S. (2001) *Trends Cardiovasc. Med.* **11,** 26–31
14. Czekay, R. P., Orlando, R. A., Woodward, L., Lundstrom, M., and Farquhar, M. G. (1997) *Mol. Biol. Cell* **8,** 517–532
15. Yuseff, M. I., Farfan, P., Bu, G., and Marzolo, M. P. (2007) *Traffic* **8,** 1215–1230
16. Phiel, C. J., Wilson, C. A., Lee, V. M., and Klein, P. S. (2003) *Nature* **423,** 435–439
17. Carro, E., Trejo, J. L., Gomez-Isla, T., LeRoith, D., and Torres-Aleman, I. (2002) *Nat. Med.* **8,** 1390–1397
18. Carro, E., Trejo, J. L., Gerber, A., Loetscher, H., Torrado, J., Metzger, F., and Torres-Aleman, I. (2006) *Neurobiol. Aging* **27,** 1250–1257
19. Larsson, M., Hjälm, G., Sakwe, A. M., Engström, A., Höglund, A. S., Larsson, E., Robinson, R. C., Sundberg, C., and Rask, L. (2003) *Biochem. J.* **373,** 381–391
20. Vardy, E. R., Rice, P. J., Bowie, P. C., Holmes, J. D., Grant, P. J., and Hooper, N. M. (2007) *J. Alzheimers Dis.* **12,** 285–290
21. Medina, M., and Castro, A. (2008) *Curr. Opin. Drug Discov. Dev.* **11,** 533–543
22. Zhai, X. Y., Nielsen, R., Birn, H., Drumm, K., Mildenberger, S., Freudinger, R., Moestrup, S. K., Verroust, P. J., Christensen, E. I., and Gekle, M. (2000) *Kidney Int.* **58,** 1523–1533
23. Trinchese, F., Liu, S., Battaglia, F., Walter, S., Mathews, P. M., and Arancio, O. (2004) *Ann. Neurol.* **55,** 801–814
24. Obermayr, R. P., Mayerhofer, L., Knechtelsdorfer, M., Mersich, N., Huber, E. R., Geyer, G., and Tragl, K. H. (2005) *Exp. Gerontol.* **40,** 157–163
25. Butovsky, O., Koronyo-Hamaoui, M., Kunis, G., Ophir, E., Landa, G., Cohen, H., and Schwartz, M. (2006) *Proc. Natl. Acad. Sci. U.S.A.* **103,** 11784–11789
26. Martinez, A., and Perez, D. I. (2008) *J. Alzheimers Dis.* **15,** 181–191
27. Chun, J. T., Wang, L., Pasinetti, G. M., Finch, C. E., and Zlokovic, B. V. (1999) *Exp. Neurol.* **157,** 194–201
28. Christensen, E. I., and Birn, H. (2002) *Nat. Rev. Mol. Cell Biol.* **3,** 256–266
29. Kappeler, L., De Magalhaes Filho, C., Dupont, J., Leneuve, P., Cervera, P., Périn, L., Loudes, C., Blaise, A., Klein, R., Epelbaum, J., Le Bouc, Y., and Holzenberger, M. (2008) *PLoS Biol.* **6,** e254
30. Watanabe, T., Miyazaki, A., Katagiri, T., Yamamoto, H., Idei, T., and Iguchi, T. (2005) *J. Am. Geriatr. Soc.* **53,** 1748–1753
31. Mustafa, A., Lannfelt, L., Lilius, L., Islam, A., Winblad, B., and Adem, A. (1999) *Dement. Geriatr. Cogn. Disord.* **10,** 446–451
32. Rivera, E. J., Goldin, A., Fulmer, N., Tavares, R., Wands, J. R., and de la Monte, S. M. (2005) *J. Alzheimers Dis.* **8,** 247–268
33. Salehi, Z., Mashayekhi, F., and Naji, M. (2008) *Biofactors* **33,** 99–106
34. Tham, A., Nordberg, A., Grissom, F. E., Carlsson-Skwirut, C., Viitanen, M., and Sara, V. R. (1993) *J. Neural Transm. Park. Dis. Dement. Sect.* **5,** 165–176